

# Calibrating Car-Following Models by Using Trajectory Data

## Methodological Study

Arne Kesting and Martin Treiber

The car-following behavior of individual drivers in real city traffic is studied on the basis of (publicly available) trajectory data sets recorded by a vehicle equipped with a radar sensor. By means of a nonlinear optimization procedure based on a genetic algorithm, the intelligent driver model and the velocity difference model are calibrated by minimizing the deviations between the observed driving dynamics and the simulated trajectory in following the same leading vehicle. The reliability and robustness of the nonlinear fits are assessed by applying different optimization criteria, that is, different measures for the deviations between two trajectories. The obtained errors are between 11% and 29%, which is consistent with typical error ranges obtained in previous studies. It is also found that the calibrated parameter values of the velocity difference model depend strongly on the optimization criterion, whereas the intelligent driver model is more robust. The influence of a reaction time is investigated by applying an explicit delay to the model input. A negligible influence of the reaction time is found and indicates that drivers compensate for their reaction time by anticipation. Furthermore, the parameter sets calibrated to a certain trajectory are applied to the other trajectories; this step allows for model validation. The results indicate that intradriver variability rather than interdriver variability accounts for a large part of the calibration errors. The results are used to suggest some criteria toward a benchmarking of car-following models.

As microscopic traffic flow models are used mainly to describe collective phenomena such as traffic breakdowns, traffic instabilities, and the propagation of stop-and-go waves, these models traditionally are calibrated with respect to macroscopic traffic data, for example, 1-min flow and velocity data collected by double-loop detectors. As microscopic traffic data have become more available, the problem of analyzing and comparing microscopic traffic flow models with real microscopic data has raised some interest in the literature (1–5).

This paper considers three empirical trajectories of different drivers that are publicly available and that have been provided by Robert Bosch GmbH (6). The data sets were recorded in 1995 during an afternoon peak period on a fairly straight one-lane road in Stuttgart, Germany. A car equipped with a radar sensor in front provides the relative speed and distance to the car ahead. The duration of the

measurements are 250 s, 400 s, and 300 s, respectively. All data sets show complex situations of daily city traffic with several acceleration and deceleration periods, including standstills caused by traffic lights. Because of their high resolution and quality, these data sets have been considered in the literature (5, 7, 8).

Two car-following models of similar complexity (thus, with the same number of parameters), are applied to the empirical trajectories: the intelligent driver model (IDM) (9) and the velocity difference model (VDIFF) (10). Nonlinear optimization will be used to determine the optimal model parameters that best fit the given data. In contrast to the previous studies, this study considers three different error measures because the fit errors alone do not provide a good basis for evaluation of the applied models. Furthermore, it is argued that it is sufficient (and superior) to minimize the objective functions exclusively with respect to vehicle gaps and not with respect to speeds. It is shown that the variation in the parameter values with respect to the different measures is surprisingly high for the VDIFF, whereas the IDM is more robust, suggesting a new criterion in the context of benchmarking microscopic traffic models. The paper also shows that an additional parameter—namely, the reaction time that is widely considered to be an important part of a car-following model—does not improve the reproduction of the empirical data. Since reaction times clearly exist, this result suggests that drivers compensate for the human reaction time by anticipation.

### CAR-FOLLOWING MODELS UNDER INVESTIGATION

Microscopic traffic models describe the motion of each individual vehicle, that is, they model the action such as accelerations and decelerations of each driver as a response to the surrounding traffic by means of an acceleration strategy toward a desired velocity in the free-flow regime, a braking strategy for approaching other vehicles or obstacles, and a car-driving strategy for maintaining a safe distance when driving behind another vehicle. Microscopic traffic models typically assume that human drivers react to the stimulus from neighboring vehicles with the dominant influence originating from the directly leading vehicle known as follow-the-leader or car-following approximation.

Two microscopic car-following models are considered that are formulated as ordinary differential equations and, consequently, space and time are treated as continuous variables. This model class is characterized by an acceleration function

$$\dot{v} = \frac{dv}{dt}$$

Institute for Transport and Economics, Technische Universität Dresden, Andreas-Schubert-Strasse 23, D-01062 Dresden, Germany. Corresponding author: A. Kesting, keasting@vwi.tu-dresden.de.

*Transportation Research Record: Journal of the Transportation Research Board*, No. 2088, Transportation Research Board of the National Academies, Washington, D.C., 2008, pp. 148–156.  
DOI: 10.3141/2088-16

that depends on the actual velocity  $v(t)$ , the (net distance) gap  $s(t)$ , and the velocity difference  $\Delta v(t)$  relevant to the leading vehicle:

$$\dot{v}(s, v, \Delta v) = f(s, v, \Delta v) \quad (1)$$

Notice that  $\Delta v$  is defined as the approaching rate, that is, positive if the following vehicle is faster than the leading vehicle.

### Intelligent Driver Model

The IDM is defined by the acceleration function (9)

$$\dot{v}_{\text{IDM}}(s, v, \Delta v) = a \left[ 1 - \left( \frac{v}{v_0} \right)^4 - \left( \frac{s^*(v, \Delta v)}{s} \right)^2 \right] \quad (2)$$

This expression combines the acceleration strategy

$$\dot{v}_{\text{free}}(v) = a \left[ 1 - \left( \frac{\dot{v}}{v_0} \right)^4 \right]$$

toward a desired velocity  $v_0$  on a free road with the parameter  $a$  for the maximum acceleration with a braking strategy

$$\dot{v}_{\text{brake}}(s, v, \Delta v) = -a \left( \frac{s^*}{s} \right)^2$$

which is dominant if the current gap  $s(t)$  to the preceding vehicle becomes smaller than the desired minimum gap:

$$s^*(v, \Delta v) = s_0 + vT + \frac{v\Delta v}{2\sqrt{ab}} \quad (3)$$

The minimum distance  $s_0$  in congested traffic is significant for low velocities only. The dominating term of Equation 3 in stationary traffic is  $vT$ , which corresponds to following the leading vehicle with a constant desired (safety) time gap  $T$ . The last term is active only in nonstationary traffic and implements an intelligent driving behavior including a braking strategy that, in nearly all situations, limits braking decelerations to the comfortable deceleration  $b$ . Note, however, that the IDM brakes stronger than  $b$  if the gap becomes too small. This braking strategy makes the IDM collision-free. All IDM parameters  $v_0$ ,  $T$ ,  $s_0$ ,  $a$ , and  $b$ , are defined by positive values.

### Velocity Difference Model

Another popular car-following model is the VDIFF (10), which is closely related to the optimal velocity model by Bando et al. (11). The acceleration function consists of a term proportional to a gap-dependent optimal velocity  $v_{\text{opt}}(s)$  and a term that takes velocity differences  $\Delta v$  as a linear stimulus into account:

$$\dot{v}_{\text{VDIFF}}(s, v, \Delta v) = \frac{v_{\text{opt}}(s) - v}{\tau} - \lambda \Delta v \quad (4)$$

The parameter  $\tau$  is the relaxation time that describes the adaptation to a new velocity due to changes in  $s$  and  $v$ . The sensitivity parameter  $\lambda$  considers the crucial influence of  $\Delta v$ . The properties of the VDIFF are defined by the function for the optimal velocity  $v_{\text{opt}}(s)$ . In the literature, the following function is proposed:

$$v_{\text{opt}}(s) = \frac{v_0}{2} \left[ \tanh \left( \frac{s}{l_{\text{int}}} - \beta \right) - \tanh(-\beta) \right] \quad (5)$$

The parameter  $v_0$  defines the desired velocity under free traffic conditions. The interaction length  $l_{\text{int}}$  determines the transition regime for the  $s$ -shaped function (Equation 5) going from  $v_{\text{opt}}(s=0) = 0$  to  $v_{\text{opt}} \rightarrow v_0$  when the distance to the leading vehicles becomes large. Finally, the form factor  $\beta$  defines (together with  $l_{\text{int}}$ ) the shape of the equilibrium flow–density relation (also known as fundamental diagram), which is considered later in the paper. In contrast to the IDM, the VDIFF exhibits collisions for some regimes of the parameter space.

## CALIBRATION METHODOLOGY

Finding an optimal parameter set for a car-following model with a nonlinear acceleration function such as Equations 2 and 4 corresponds to a nonlinear optimization problem which has to be solved numerically.

### Simulation Setup

The Bosch trajectory data contains velocities of both the leading and the following (measuring) vehicle (6). These data therefore allow for a direct comparison between the measured driver behavior and trajectories simulated by a car-following model with the leading vehicle serving as externally controlled input. Initialized with the empirically given distance and velocity differences,  $v^{\text{sim}}(t=0) = v^{\text{data}}(0)$  and  $s^{\text{sim}}(t=0) = s^{\text{data}}(0)$ , the microscopic model is used to compute the acceleration and, from this, the trajectory of the following car. The gap to the leading vehicle is then given by the difference between the simulated trajectory  $x^{\text{sim}}(t)$  (front bumper) and the given position of the rear bumper of the leading vehicle  $x_{\text{lead}}^{\text{data}}(t)$ :

$$s^{\text{sim}}(t) = x_{\text{lead}}^{\text{data}}(t) - x^{\text{sim}}(t) \quad (6)$$

This can be directly compared to the gap  $s^{\text{data}}(t)$  provided by the Bosch data (6). In addition, the distance  $s^{\text{sim}}(t)$  has to be reset to the value in the data set when the leading object changes as a result of a lane change by one of the considered vehicles. For example, the leading vehicle of Data Set 3 (see the results section) turning into another street at about 144 s leads to a jump in the gap of the considered follower.

### Objective Functions

The calibration process aims at minimizing the difference between the measured driving behavior and the driving behavior simulated by the car-following model under consideration. Basically, any quantity can be used as an error measure that is not fixed in the simulation, such as the velocity, the velocity difference, or the gap. In the following, the error in the gap  $s(t)$  is used for conceptual reasons: when optimizing with respect to  $s$ , the average velocity errors are automatically reduced as well. This does not hold the other way around, as the error in the distance may incrementally grow when optimizing with respect to differences in the velocities  $v^{\text{sim}}(t)$  and  $v_{\text{follow}}^{\text{data}}(t)$ .

For the parameter optimization, an objective function is needed as a quantitative measure of the error between the simulated and observed trajectories. As the objective function has a direct impact on the

calibration result, three different error measures are considered. The relative error is defined as a functional of the empirical and simulated time series,  $s^{\text{data}}(t)$  and  $s^{\text{sim}}(t)$ :

$$F_{\text{rel}}[s^{\text{sim}}] = \sqrt{\left\langle \left( \frac{s^{\text{sim}} - s^{\text{data}}}{s^{\text{data}}} \right)^2 \right\rangle} \quad (7)$$

Here, the expression  $\langle \cdot \rangle$  means the temporal average of a time series of duration  $\Delta T$ , that is,

$$\langle z \rangle := \frac{1}{\Delta T} \int_0^{\Delta T} z(t) dt \quad (8)$$

Since the relative error is weighted by the inverse distance, this measure is more sensitive to small distances  $s$  than to large distances. For example, a simulated gap of 10 m compared to a distance of 5 m in the empirical data results in a large error of 100%, whereas the same deviation of 5 m leads, for instance, to an error of 5% only for a spacing of 100 m, which is typical for large velocities. In addition, absolute error is defined as

$$F_{\text{abs}}[s^{\text{sim}}] = \sqrt{\frac{\left\langle (s^{\text{sim}} - s^{\text{data}})^2 \right\rangle}{\left\langle s^{\text{data}} \right\rangle^2}} \quad (9)$$

As the denominator is averaged over the whole time series interval, the absolute error  $F_{\text{abs}}[s^{\text{sim}}]$  is less sensitive to small deviations from the empirical data than  $F_{\text{rel}}[s^{\text{sim}}]$ . However, the absolute error measure is more sensitive to large differences in the numerator, that is, for large distances  $s$ . Note that the error measures are normalized to make them independent of the duration  $\Delta T$  of the considered time series allowing for a direct comparison of different data sets.

Because the absolute error systematically overestimates errors for large gaps (at high velocities) and the relative error systematically overestimates deviations of the observed headway in the low velocity range, a combination of both error measures is also studied. To do this, the mixed error measure is defined:

$$F_{\text{mix}}[s^{\text{sim}}] = \sqrt{\frac{1}{\left\langle |s^{\text{data}}| \right\rangle} \left\langle \frac{(s^{\text{sim}} - s^{\text{data}})^2}{|s^{\text{data}}|} \right\rangle} \quad (10)$$

### Optimization with Genetic Algorithm

To find an approximative solution to the nonlinear optimization problem, a genetic algorithm is applied as a search heuristic (12). The implemented genetic algorithm proceeds as follows:

1. An individual represents a parameter set of a car-following model, and a population consists of  $N$  such sets.
2. In each generation, the fitness of each individual in the population is determined via one of the objective functions, Equation 7, 9, or 10.
3. Pairs of two individuals are stochastically selected from the current population on the basis of their fitness scores and recombined to generate a new individual. Except for the best individual, which is kept without any modification to the next generation, the genes of all individuals, that is, their model parameters, are varied randomly, corresponding to a mutation that is controlled by a given probability. The resulting new generation is then used in the next iteration.

4. The termination criterion is implemented as a two-step process. Initially, a fixed number of generations is evaluated. Then, the evolution terminates after convergence, which is specified by a constant best-of-generation score for at least a given number of generations.

### Parameter Constraints and Collision Penalty

Both the IDM and the VDIFF contain five parameters and are therefore formally equivalent in their complexity. To restrict the parameter space for the optimization to reasonable and positive parameter values without excluding possible solutions, the following constraints are applied for the minimum and maximum values. For the IDM, the desired velocity  $v_0$  is restricted to the interval [1, 70] m/s, the desired time gap  $T$  to [0.1, 5] s, the minimum distance  $s_0$  to [0.1, 8] m, and the maximum acceleration  $a$  and the comfortable deceleration  $b$  to [0.1, 6] m/s<sup>2</sup>. For the VDIFF, the allowed parameter intervals are also [1, 70] m/s for the desired velocity  $v_0$ , [0.05, 20] s for the relaxation time  $\tau$ , [0.1, 100] m for the interaction length  $l_{\text{int}}$ , and [0.1, 10] m for the form factor  $\beta$ , and the (unitless) sensitivity parameter  $\lambda$  is limited to [0, 3].

Finally, it must be taken into account that some regions of the VDIFF parameter space lead to collisions. To make these solutions unattractive to the optimization algorithm, a large crash penalty value is added to the objective measure, which is the standard procedure for numerical optimization.

## CALIBRATION RESULTS

### Optimal Model Parameters

By applying the described optimization method, the best fit of the car-following models to the empirical data is found. The calibration results for the three data sets and the considered three objective functions, Equations 7, 9, and 10, are summarized in Table 1. Figure 1 compares the dynamics of the gap  $s(t)$  resulting from the calibrated parameters with the empirically measured trajectories. The depicted simulations have been carried out with the optimal parameters regarding the mixed error measure, Equation 10. The obtained errors are in the range of 11% to 29%, which is consistent with typical error ranges obtained in previous studies (1–3). The concluding section discussed the influencing factors for the deviations between empirical and simulated car-following behavior.

Obviously, the calibrated model parameters vary from one data set to another because of different driving situations. Furthermore, a model that best fits a certain driver does not necessarily do so for a different driver. In Data Set 3, the IDM performs considerably better than the VDIFF, whereas little difference is found for Data Set 2. Moreover, the calibrated model parameters also depend considerably on the underlying objective function. For example, Data Set 3 can be reproduced best, and Data Set 2 leads to the largest deviations—consistently for both the IDM and the VDIFF. Here, the IDM parameters show a significantly smaller variation for a considered data set than does the VDIFF. This finding is relevant for a benchmarking of traffic models. It is not sufficient to consider only the fit errors, but the quality of the traffic model is also determined by the consistency and robustness of the calibrated parameters. A subsequent section studies the models' parameter spaces by means of a sensitivity and validation analysis.

In Data Set 3, the desired speed is estimated to be  $v_0 = 58.0$  km/h (corresponding to the maximum velocity reached in the recorded driving situations), whereas the other two sets result in  $v_0 \approx 250$  km/h

TABLE 1 Calibration Results for Models

	Data Set 1			Data Set 2			Data Set 3		
	$F_{rel}(s)$	$F_{mix}(s)$	$F_{abs}(s)$	$F_{rel}(s)$	$F_{mix}(s)$	$F_{abs}(s)$	$F_{rel}(s)$	$F_{mix}(s)$	$F_{abs}(s)$
<b>IDM</b>									
Error [%]	24.0	20.7	20.7	28.7	26.2	25.6	18.0	13.0	11.2
$v_0$ [m/s]	70.0	69.9	70.0	69.8	69.9	69.9	16.1	16.1	16.4
$T$ [s]	1.07	1.12	1.03	1.51	1.43	1.26	1.30	1.30	1.39
$s_0$ [m]	2.41	2.33	2.56	2.63	2.82	3.40	1.61	1.52	1.04
$a$ [m/s <sup>2</sup> ]	1.00	1.23	1.40	0.956	0.977	1.06	1.58	1.56	1.52
$b$ [m/s <sup>2</sup> ]	3.21	3.20	3.73	0.910	0.994	1.11	0.756	0.633	0.614
<b>VDIFF</b>									
Error [%]	25.5	25.8	21.4	29.1	26.7	25.6	28.2	19.0	14.5
$v_0$ [m/s]	7.02	14.8	18.1	11.7	49.5	9.56	70.0	26.3	46.2
$\tau$ [s]	11.9	20.0	4.90	1.48	20.0	20.0	19.4	4.87	5.45
$l_{int}$ [m]	1.62	9.60	5.23	3.93	12.1	4.26	28.6	20.7	40.9
$\beta$ [m]	4.16	1.21	2.14	2.69	1.89	2.30	1.31	0.758	0.102
$\lambda$ [1]	0.534	0.724	0.536	0.00	0.610	0.579	0.59	0.694	0.610

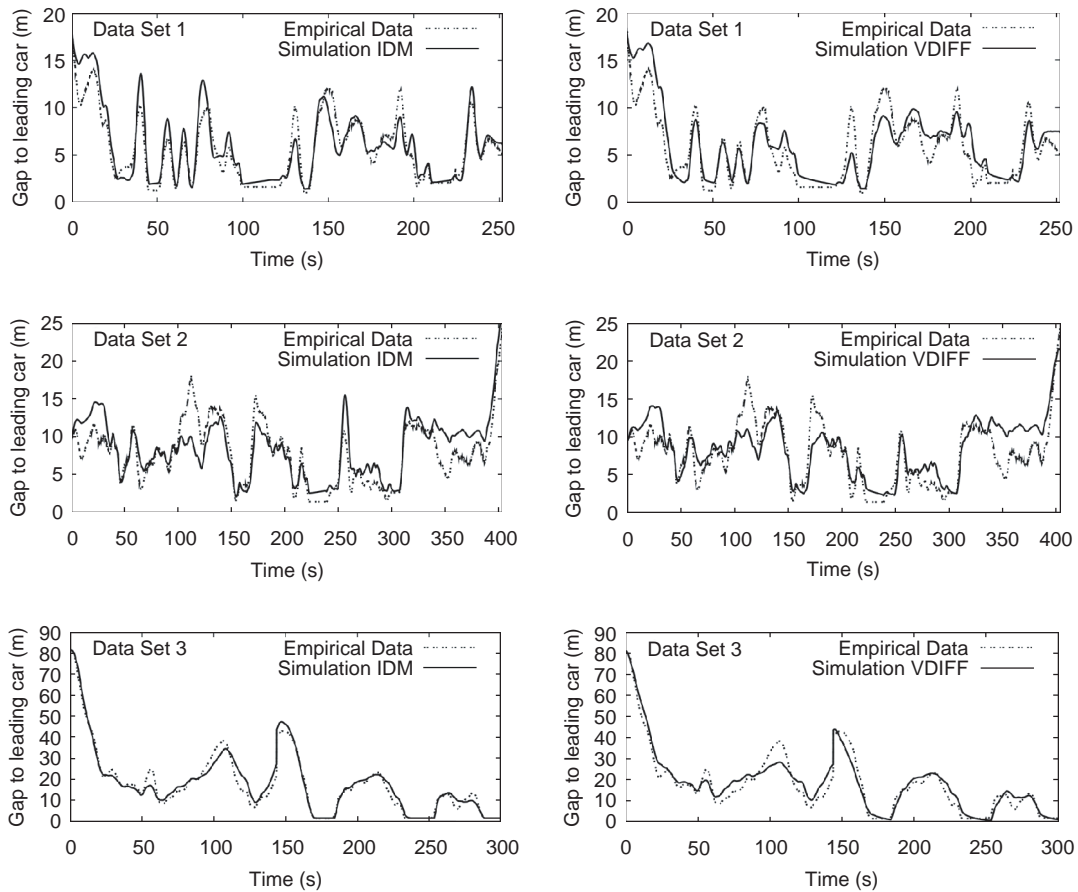


FIGURE 1 Comparison of simulated and empirical trajectories. Model parameters are calibrated according to Table 1 for mixed error measure.

(corresponding to the maximum value allowed in the numerical optimization). This unreasonably high value can be explained by the fact that Data Sets 1 and 2 describe bound traffic without acceleration periods to the desired speed. Therefore, the calibration result of  $v_0$  is relevant only for a lower bound. This is plausible because the derived velocity does not influence the driving dynamics if it is considerably higher than  $v_{lead}$  in a car-following situation. Consistent with this, the error measures for Data Sets 1 and 2 change little when varying  $v_0$  in the range between 60 and 250 km/h.

### Microscopic Flow–Density Relations

In the literature, the state of traffic is often formulated in macroscopic quantities such as traffic flow and density. The translation from the microscopic gap  $s$  into the density  $\rho$  is given by the micro–macro relation

$$\rho(s) = \frac{1}{s+l} \tag{11}$$

where  $l$  is the vehicle length, fixed here to 5 m. The flow  $Q$  as defined by the inverse of the time headway is given by the vehicle’s actual time gap  $\frac{s}{v}$  and the passage time for its own vehicle length  $\frac{l}{v}$ :

$$Q(s,v) = \frac{v}{s+l} \tag{12}$$

Furthermore, the flow–density points  $(Q(t), \rho(t))$  can be contrasted to the models’ equilibrium properties describing states of homoge-

neous and stationary traffic (so-called fundamental diagrams). As equilibrium traffic is defined by vanishing velocity differences and accelerations, the modeled drivers keep a constant velocity  $v_e$ , which depends on the gap to the leading vehicle. For the VDIFF, this equilibrium velocity is directly given by the optimal velocity function, Equation 5. Hence, the fundamental diagram  $Q(\rho) = v_e \rho$  can be directly calculated by using Equation 11. For the IDM under the conditions  $\dot{v} = 0$  and  $\Delta v = 0$ , only the inverse, that is, the equilibrium gap  $s_e$  as a function of the velocity, can be solved analytically, leading to

$$s_e(v) = \frac{s_0 + vT}{\sqrt{1 - \left(\frac{v}{v_0}\right)^4}} \tag{13}$$

However, the fundamental diagrams of the IDM can be obtained numerically by parametric plots varying  $v$ .

Figure 2 is an alternative view to Figure 1 of empirical and simulated data, for traffic stability in particular. The flow–density points  $(Q(t), \rho(t))$  are plotted for each recorded time step of the empirical data and the simulated trajectories. In addition, the fundamental diagram is plotted as an equilibrium curve. The diagrams give a good overview of the recorded traffic situations. Whereas Data Sets 1 and 2 mainly contain car-following behavior at distances smaller than 20 m (corresponding to densities larger than 50/km), Data Set 3 also features a nonrestricted driving situation with a short period of free acceleration (corresponding to the branch with densities lower than 30/km of the flow–density plot). Furthermore, the plots directly show the stability properties of the found optimal parameter sets. Straight lines (for example, in Data Sets 1 and 2 for the VDIFF) correspond to very stable settings with short velocity adaptation times  $\tau$ , whereas wide

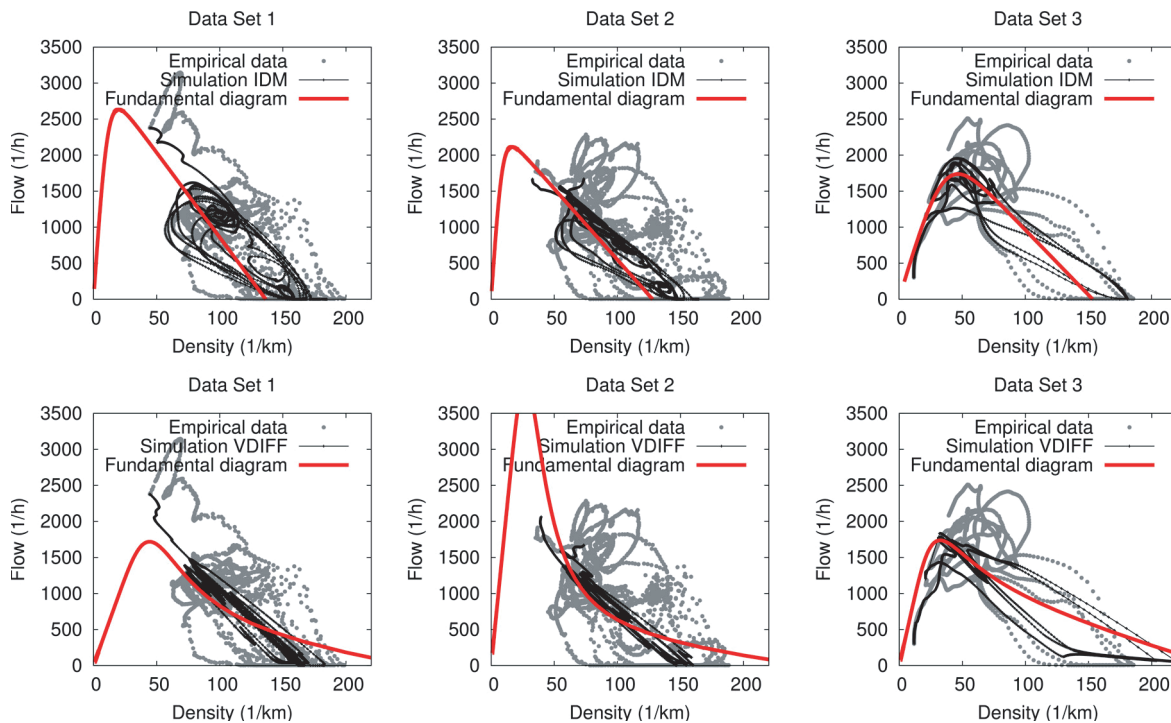


FIGURE 2 Microscopic flow–density relations derived from given and simulated gaps  $s(t)$  and velocities  $v(t)$ , respectively. Equilibrium flow–density relations are also plotted. Representation offers alternative view to Figure 1 of empirical and simulated data, for traffic stability in particular.

circles around the equilibrium state (as for the IDM in Data Set 1) indicate less stable settings corresponding to smaller values of the IDM acceleration parameter  $a$ . Both parameters are related inversely to each other: a large relaxation time  $\tau$  in the VDIFF corresponds to a small value of  $a$  in the IDM.

### Sensitivity Analysis

Starting from the optimized model parameters summarized in Table 1, varying a single model parameter while keeping the other parameters constant is straightforward. The resulting one-dimensional scan of the parameter space gives good insight into the model's parameter properties and sensitivity. Furthermore, the application of different objective functions such as Equations 7, 9, and 10 can be seen as a benchmark for the robustness of the model calibration. A good model should not strongly depend on the chosen error measure.

Figure 3 shows the resulting error measures of Data Set 3, plotted in logarithmic scale. Remarkably, all error curves for the IDM are smooth and show only one minimum (which is therefore easy to determine by the optimization algorithm). As the data sets mainly describe car-following situations in obstructed traffic and standstills, the IDM parameters  $T$ ,  $s_0$ , and  $a$  are particularly significant and show distinct minima for the three proposed error measures, whereas the values of  $v_0$  were difficult to determine exactly from Data Sets 1 and 2, where the desired velocity is never approximated. The comfortable deceleration  $b$  also is not very distinct (not shown here). The solutions belonging to different objective functions are altogether in the same parameter range. This robustness of the IDM parameter space is an important finding of this study.

The results for the VDIFF imply a less positive model assessment: the calibration results strongly vary with the chosen objective function, indicating a strong sensitivity of the model parameters. Furthermore, too high values of the desired velocity lead to vehicle collisions in the simulation, as indicated by an abrupt raise in the error curves. Interestingly, the sensitivity parameter  $\lambda$  (taking into account velocity differences) has to be larger than approximately 0.5 to avoid accidents. Velocity differences are therefore a crucial input quantity for car-following models.

### Consideration of Explicit Reaction Time

The considered car-following models describe an instantaneous reaction (in the acceleration) to the leading car. A complex reaction time, however, is an essential feature of human driving because of the physiological aspects of sensing, perceiving, deciding, and performing an action. Therefore, a reaction time is incorporated into the IDM and the VDIFF to investigate whether an additional model parameter will improve the calibration results.

A reaction time  $T_r$  can be additionally incorporated in a time-continuous model of Type 1 by evaluating the right-hand side at a previous time  $t - T_r$ . If the reaction time is a multiple of the update time interval,  $T_r = n\Delta t$ , it is straightforward to consider all input quantities at  $n$  time steps in the past. If  $T_r$  is not a multiple of the update time interval  $\Delta t$ , a linear interpolation proposed by Treiber et al. (13) is used according to

$$x(t - T_r) = \beta x_{t-n-1} + (1 - \beta)x_{t-n} \quad (14)$$

where  $x$  denotes any input quantity such as  $s$ ,  $v$ , or  $\Delta v$  (see the right-hand side of Equation 1), and  $x_{t-n}$  denotes this quantity taken  $n$  time steps before the actual step. Here,  $n$  is the integer part of  $T_r/\Delta t$  and the weight factor of the linear interpolation is given by  $\beta = T_r/\Delta t - n$ . As initial conditions, values for the dependent variables are required for a whole time interval  $T_r$ . In the simulations, the values from the empirical data were used as initial conditions. For the stability properties of the IDM with reaction time, see the work of Kesting and Treiber (14).

Figure 4 shows the systematic variation of the reaction time  $T_r$ , while the other parameters are kept at their optimal values as listed in Table 1 for the mixed error measure, Equation 10. An additional reaction time  $T_r$  does not decrease the fit errors. Moreover, for small reaction times, there is no influence at all, whereas values larger than a critical reaction time cause collisions as indicated by the abrupt raise in the errors. For the IDM, this critical reaction time  $T_c^{\text{crit}}$  is smaller but of the order of the calibrated desired (safety) time gap parameters for the three sets. Similar values have been found for the VDIFF. Because the VDIFF does not feature an explicit time gap parameter, however, it is not as easy to interpret.

The values of  $T_c^{\text{crit}}$  are relatively high because the considered scenarios are limited to a single pair of vehicles over a limited duration and therefore only local stability properties can be tested. This finding is in agreement with a simulation study on local and collective stability properties of the IDM with explicit delay (14, 15). Furthermore, the negligible influence of the reaction time as an explanatory variable can be interpreted in the way the human drivers are able to compensate for their considerable reaction time, which is about 1 s (16), by anticipation, because of driving experience. These compensating influences have recently been modeled and analyzed (13, 14).

### Validation by Cross Comparison

The obtained calibrated parameters are validated by applying these settings to the other data sets, that is, by using the parameters calibrated on the basis of another data set. The three optimal parameter settings listed in Table 1 are used with the mixed error measure (Equation 10). The obtained errors can be found in Table 2.

This cross-comparison allows one to check for the reliability of the obtained parameters and automatically takes into account the variance of the calibrated parameter values. For the IDM, the obtained errors for the cross-compared simulation runs are of the same order as for the calibrated parameter sets. Therefore, the car-following behavior of the IDM turned out to be robust for reasonable changes of parameter settings. In contrast, the VDIFF is more sensitive, leading to larger errors. One parameter set even led to collisions, which is reflected in a large error due to the applied crash penalty.

### DISCUSSION AND CONCLUSIONS

The IDM and the VDIFF were used to reproduce three empirical trajectories. Calibration errors were found to be between 11% and 30%. These results are consistent with typical error ranges obtained in previous studies (1, 2, 3). Three qualitative influences contribute to these deviations between observation and reproduction. Note, however, that noise in the data contribute to the fit errors as well (17).

A significant part of the deviations between measured and simulated trajectories can be attributed to the interdriver variability (18),

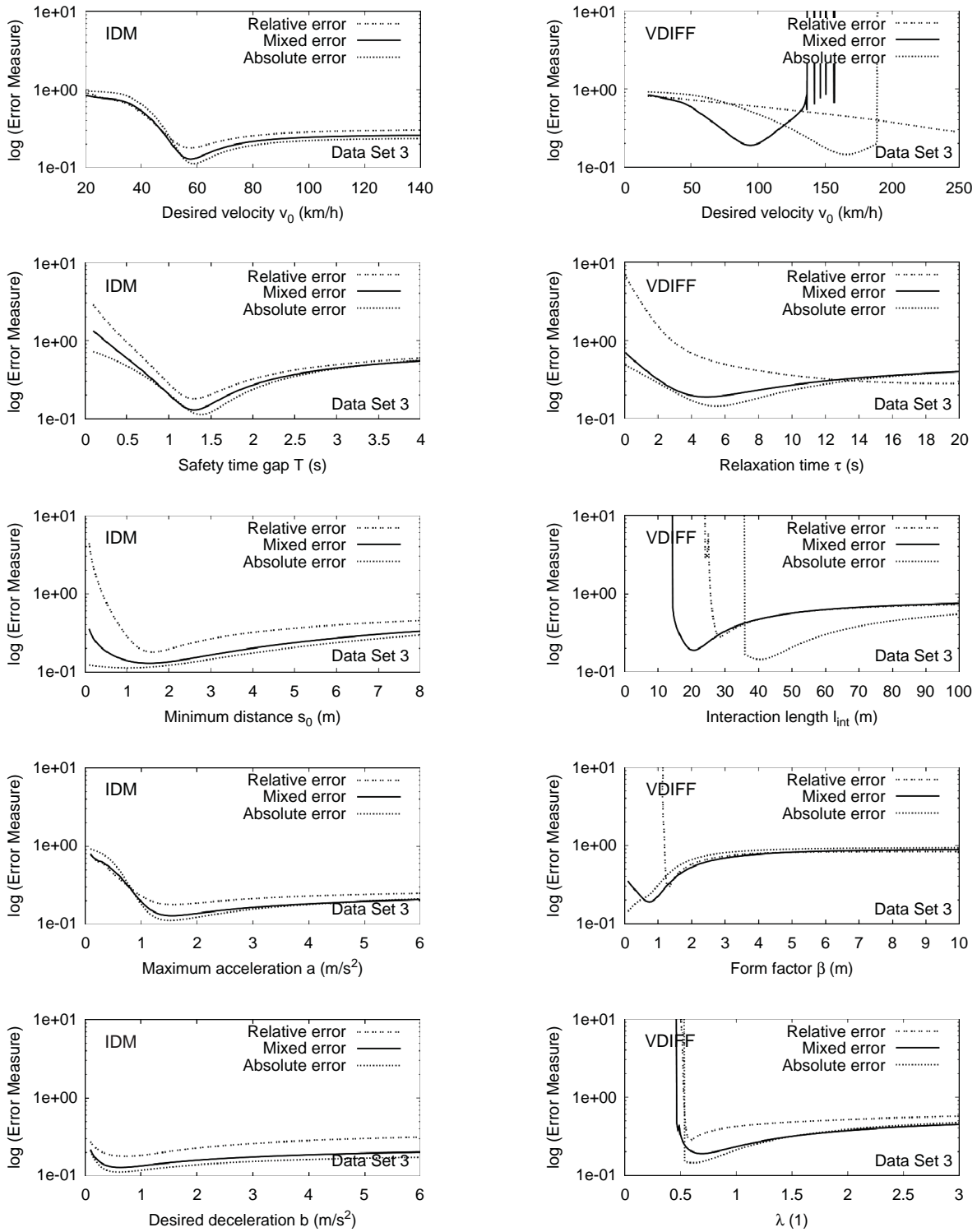


FIGURE 3 Systematic variation of one model parameter while other parameters are kept at optimal values listed in Table 1. Diagrams show considered error measures of Equations 7, 9, and 10 for IDM and VDIFF using Data Set 3. The errors are plotted in logarithmic scale.

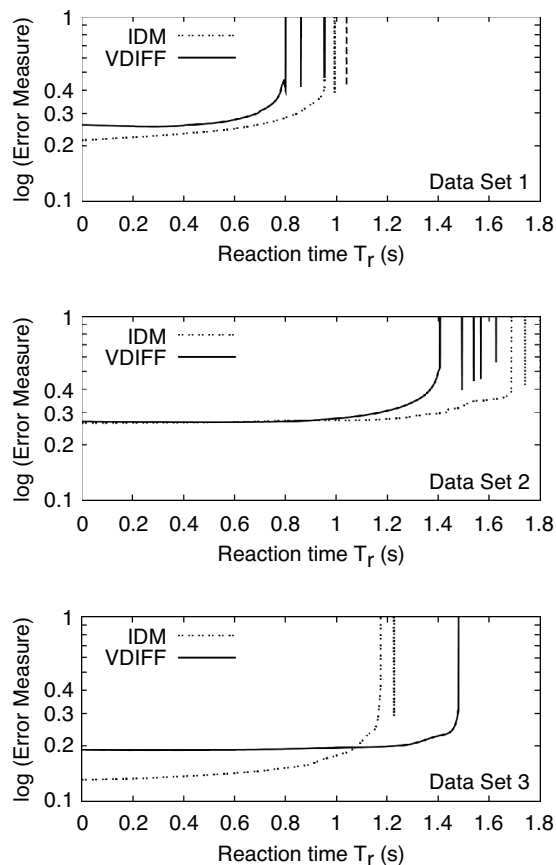


FIGURE 4 Systematic variation of reaction time  $T_r$  that has been explicitly incorporated in IDM and VDIFF. Reaction time  $T_r$  has only small influence for values well below desired (safety) time gap  $T$ , which is an explicit model parameter of IDM but only implicitly implemented in VDIFF. Higher reaction times lead to collisions, resulting in rapidly growing errors because of numerical penalties.

as has been shown by cross-comparison. Microscopic traffic models can easily cope with this kind of heterogeneity because different parameter values can be attributed to each individual driver-vehicle unit. However, to obtain these distributions of calibrated model parameters, more trajectories have to be analyzed, for example, by using the NGSIM trajectory data (19).

A second contribution to the overall calibration error results from a nonconstant driving style of human drivers, which is referred to as intradriver variability: human drivers do not drive constantly over

time, that is, their behavioral driving parameters are time dependent. For a first estimation, the distances at standstills in Data Set 3 were compared to the minimum distance as a direct model parameter of the IDM. The driver stops three times because of red traffic lights. The bumper-to-bumper distances are  $s_{\text{stop},1} = 1.39\text{m}$ ,  $s_{\text{stop},2} = 1.42\text{m}$ , and  $s_{\text{stop},3} = 1.64\text{m}$ . These different values in similar situations indicate that a deterministic car-following model only allows for an averaged, thus, effective description of the human driving behavior, resulting in parameter values that capture the mean observed driving performance. Considering the theoretical best case of a perfect agreement between data and simulation for all times except for the three standstills, the relative error function depends on  $s_0$  only, and an analytical minimization of  $s_0$  results in  $s_0^{\text{opt}} \approx 1.458\text{m}$ . This optimal solution defines a theoretical lower bound (based on about 15% of the data of the considered time series) for the relative error measure of  $\xi_{\text{min}}(s_0^{\text{opt}}) \approx 7.9\%$ . Therefore, the intradriver variability accounts for a large part of the deviations between simulations and empirical observations. This influence could be captured by considering time-dependent model parameters reflecting driver adaptation processes as for example proposed in (20, 21).

Finally, driver anticipation contributes to the overall error as well but is not incorporated in simple car-following models. This is one possible cause for a model error, that is, the residual difference between a perfectly time-independent driving style and a model calibrated to it. For example, the study found a negligible influence of the additionally incorporated reaction time, indicating that human drivers very well anticipate while driving and therefore compensate for their physiological reaction time. However, these physiological and psychological aspects can be determined only indirectly, by looking at the resulting driving behavior. Consequently, it would be interesting to check if a negative reaction (or, rather, anticipation) time decreases the calibration errors. More complex microscopic traffic models try to take those aspects into account (13). However, multi-leader anticipation requires trajectory data because the data recording by using radar sensors of single floating cars is limited to the immediate predecessor (22).

ACKNOWLEDGMENT

The authors thank Dirk Helbing for his review of the manuscript and for discussions.

REFERENCES

1. Brockfeld, E., R. D. Kühne, and P. Wagner. Calibration and Validation of Microscopic Traffic Flow Models. In *Transportation Research Record: Journal of the Transportation Research Board, No. 1876*, Transportation Research Board of the National Academies, Washington, D.C., 2004, pp. 62–70.
2. Ranjitkar, P., T. Nakatsuji, and M. Asano. Performance Evaluation of Microscopic Flow Models with Test Track Data. In *Transportation Research Record: Journal of the Transportation Research Board, No. 1876*, Transportation Research Board of the National Academies, Washington, D.C., 2004, pp. 90–100.
3. Punzo, V., and F. Simonelli. Analysis and Comparison of Microscopic Flow Models with Real Traffic Microscopic Data. In *Transportation Research Record: Journal of the Transportation Research Board, No. 1934*, Transportation Research Board of the National Academies, Washington, D.C., 2005, pp. 53–63.
4. Ossen, S., and S. P. Hoogendoorn. Car-Following Behavior Analysis from Microscopic Trajectory Data. In *Transportation Research Record: Journal of the Transportation Research Board, No. 1934*, Transportation

TABLE 2 Cross Comparison of Calibrated Parameters for Mixed Error Measure

Model	Data Set	Calib. Set 1 (%)	Calib. Set 2 (%)	Calib. Set 3 (%)
IDM	Set 1	20.7	28.8	28.7
	Set 2	35.2	26.2	40.1
	Set 3	41.1	27.0	13.0
VDIFF	Set 1	25.8	64.3	40.5
	Set 2	28.8	26.7	39.6
	Set 3	57.0	3,840	19.0

- Research Board of the National Academies, Washington, D.C., 2005, pp. 13–21.
5. Hoogendoorn, S., S. Ossen, and M. Schreuder. Adaptive Car-Following Behavior Identification by Unscented Particle Filtering. Presented at 86th Annual Meeting of the Transportation Research Board, Washington, D.C., 2007.
  6. *Deutsches Zentrum für Luft- und Raumfahrt*. www.dlr.de/cs/. Accessed May 5, 2007.
  7. Fouladvand, M. E., and A. H. Darooneh. Statistical Analysis of Floating-Car Data: An Empirical Study. *European Physical Journal B*, Vol. 47, 2005, pp. 319–328.
  8. Panwai, S., and H. Dia. Comparative Evaluation of Microscopic Car-Following Behavior. *IEEE Transactions on Intelligent Transportation Systems*, Vol. 6, 2005, pp. 314–325.
  9. Treiber, M., A. Hennecke, and D. Helbing. Congested Traffic States in Empirical Observations and Microscopic Simulations. *Physical Review E*, Vol. 62, 2000, pp. 1805–1824.
  10. Jiang, R., Q. Wu, and Z. Zhu. Full Velocity Difference Model for a Car-Following Theory. *Physical Review E*, Vol. 64, 2001, p. 017101.
  11. Bando, M., K. Hasebe, A. Nakayama, A. Shibata, and Y. Sugiyama. Dynamical Model of Traffic Congestion and Numerical Simulation. *Physical Review E*, Vol. 51, 1995, pp. 1035–1042.
  12. Goldberg, D. E. *Genetic Algorithms in Search, Optimization, and Machine Learning*. Addison-Wesley, Reading, Mass., 1989.
  13. Treiber, M., A. Kesting, and D. Helbing. Delays, Inaccuracies and Anticipation in Microscopic Traffic Models. *Physica A*, Vol. 360, 2006, pp. 71–88.
  14. Kesting, A., and M. Treiber. How Reaction Time, Update Time and Adaptation Time Influence the Stability of Traffic Flow. *Computer-Aided Civil and Infrastructure Engineering*, Vol. 23, 2008, pp. 125–137.
  15. Treiber, M., A. Kesting, and D. Helbing. Influence of Reaction Times and Anticipation on the Stability of Vehicular Traffic Flow. In *Transportation Research Record: Journal of the Transportation Research Board, No. 1999*, Transportation Research Board of the National Academies, Washington, D.C., 2007, pp. 23–29.
  16. Green, M. How Long Does It Take to Stop? Methodological Analysis of Driver Perception–Brake Times. *Transportation Human Factors*, Vol. 2, 2000, pp. 195–216.
  17. Ossen, S., and S. P. Hoogendoorn. Validity of Trajectory-Based Calibration Approach of Car-Following Models in the Presence of Measurement Errors. In *Transportation Research Record: Journal of the Transportation Research Board, No. 2088*, Transportation Research Board of the National Academies, Washington, D.C., 2008, pp. 117–125.
  18. Ossen, S., S. P. Hoogendoorn, and B. G. Gorte. Inter-Driver Differences in Car-Following: A Vehicle Trajectory Based Study. In *Transportation Research Record: Journal of the Transportation Research Board, No. 1965*, Transportation Research Board of the National Academies, Washington, D.C., 2007, pp. 121–129.
  19. NGSIM: Next Generation Simulation. FHWA, U.S. Department of Transportation. www.ngsim.fhwa.dot.gov. Accessed May 5, 2007.
  20. Treiber, M., and D. Helbing. Memory Effects in Microscopic Traffic Models and Wide Scattering in Flow-Density Data. *Physical Review E*, Vol. 68, 2003, p. 046119.
  21. Treiber, M., A. Kesting, and D. Helbing. Understanding Widely Scattered Traffic Flows, the Capacity Drop, and Platoons as Effects of Variance-Driven Time Gaps. *Physical Review E*, Vol. 74, 2006, p. 016123.
  22. Hoogendoorn, S., S. Ossen, and M. Schreuder. Empirics of Multianticipative Car-Following Behavior. In *Transportation Research Record: Journal of the Transportation Research Board, No. 1965*, Transportation Research Board of the National Academies, Washington, D.C., 2006, pp. 112–120.

---

*The Traffic Flow Theory and Characteristics Committee sponsored publication of this paper.*